IEEE Access
Multidisciplinary | Rapid Review | Open Access Journal

Received June 20, 2019, accepted July 2, 2019, date of publication July 5, 2019, date of current version July 23, 2019.

Digital Object Identifier 10.1109/ACCESS.2019.2927178

Performance Evaluation of Encoded Opportunistic Transmission Schemes

NATHALY OROZCO GARZÓN[1], (Member, IEEE), HENRY CARVAJAL MORA[1], (Member, IEEE), AND CELSO DE ALMEIDA[2]

[1]Telecommunications Engineering, Faculty of Engineering and Applied Sciences (FICA), Universidad de Las Américas, Quito 170125, Ecuador
[2]School of Electrical and Computer Engineering, University of Campinas, Campinas 13083-852, Brazil

Corresponding author: Nathaly Orozco Garzón (nathaly.orozco@udla.edu.ec)

This work was supported by the Universidad de Las Américas (UDLA), Quito-Ecuador, as a part of the Research Project ERT.HCM.19.01.

ABSTRACT The performance of encoded opportunistic transmission schemes in wireless channels affected by Rayleigh fading and additive white Gaussian noise (AWGN) is analyzed. In opportunistic transmission, the information is transmitted only when the fading amplitude is above a threshold. For this, the receiver with the knowledge of the channel state information notifies the instants the transmitter should transmit. Opportunistic systems with convolutional error correcting codes or with trellis coded modulation are analyzed in terms of closed-form bit error rate (BER) expressions. Nevertheless, the approach presented can be employed with any kind of error correcting codes. Hence, the performance of turbo codes is also presented in the simulations. Monte Carlo simulations verify the accuracy of the derived expressions and provide insights on the system performance. Performance results show that uncoded and encoded opportunistic systems are superior to uncoded and encoded ordinary systems (non-opportunistic), respectively. In particular, the BER curves of the opportunistic system decay exponentially when the signal-to-noise ratio (SNR) increases. On the other hand, BER curves for ordinary transmission decay linearly, where the slope is proportional to the diversity that depends on the error correcting code. Thus, opportunistic systems require less SNR to guarantee the same BER of ordinary transmission. The BER gain increases as the SNR increases. It is also observed that uncoded opportunistic systems are even superior to encoded ordinary ones. The results are validated guaranteeing the same spectral efficiency for all the scenarios. Finally, due to the exponential decay of the BER curves, coding gain expressions, used in ordinary systems over AWGN, can be used as approximations for opportunistic transmission in fading channels.

INDEX TERMS Wireless communication, opportunistic transmission, error correction codes, bit error rate, Rayleigh channels.

I. INTRODUCTION

Wireless communication research aims to improve the system performance and to employ the channel resources in an efficient manner. Important performance indicators of those researches are the bit error rate (BER) and the spectral efficiency [1]–[3].

A well-known technique to improve wireless systems performance is error correction employing codes. Error correcting codes (ECC) add redundancy to the original message so that the receiver is able to correct errors produced by the channel. Thus, BER is improved at a cost in spectral efficiency. ECC are crucial for real-time applications where resending messages is not possible [4]–[6]. Different ECC have been proposed in the literature. Among them appear the convolutional codes [7]–[9] and trellis coded modulation (TCM) [10]–[12]. In both techniques, the receiver employs a trellis decoding, which allows a maximum likelihood decoding with low complexity [11]. Typically, convolutional codes are employed with binary modulations as binary-phase-shift-keying (BPSK) [13]–[16]. Moreover, TCM uses high order modulations, as multilevel quadrature-amplitude-modulations (M-QAM), in order to compensate for spectral efficiency losses produced by the redundancy increasing.

Although in the literature there are more powerful error correction codes such as turbo codes [17],

The associate editor coordinating the review of this manuscript and approving it for publication was Mauro Fadda.

low-density-parity-check (LDPC) codes [18] or polar codes [19], the majority of times, they are evaluated through simulations [20]–[22] because it is not straightforward to find expressions to evaluate their performance in different scenarios. On the other hand, both convolutional codes and TCM codes enable a mathematical modeling that allows to find closed form-expressions to evaluate the mean BER, so that its performance is still analyzed in different operating scenarios [3], [23]. Additionally, this type of error correction codes are considered in some works related to fifth generation (5G) mobile systems [24], [25].

There are other techniques to improve the performance of wireless systems and among these techniques appear transmission schemes that take advantage of the random nature of the communications channel. Thus, this type of transmission aims the wireless channel works in favor of the system performance. One of these schemes is named as opportunistic transmission or only opportunistic transmission [26]. With this approach, the transmission is made only when the fading amplitude[1] is above a threshold value. This opportunistic transmission method improves the system performance considerably at the cost of a spectral efficiency reduction because there is no transmissions intervals. However, due to the enhanced system performance, it is possible to use higher order modulations to compensate for this loss. On the other hand, these non-transmission periods are also an interesting opportunity for cognitive networks that use the interweave technique [27], since secondary users can transmit in the non-transmission periods of primary users in the network.

In [28], opportunistic transmission is employed in wireless sensor networks scenarios. In this case, the strategy is that each sensor, with a constrained average transmission power, should save power when its channel is poor (low fading amplitude) and act when opportunities arise. The system performance is evaluated via the sum rate capacity considering uncoded scenarios. The results show that as the SNR increases, the number of active sensors can be reduced due to the opportunistic transmission employed. However, a BER analysis is not performed in this work. Another work employing opportunistic transmission is presented in [29]. Specifically, the receiver uses an antenna array and the opportunism is applied when the combiner takes only signals affected by high fading amplitudes, or equivalently, fading amplitudes above a threshold value. The system performance is evaluated in terms of the mean BER. Closed-form approximate expressions are derived in order to calculate this performance indicator. Results show that the system diversity increases significantly for each receiving antenna that is placed in the array at the receiver. In addition, in [30], the authors consider a K-user bursty Rayleigh fading interference channel, where each user transmits data intermittently with a certain probability under the local channel state information assumption. For this, it is considered an opportunistic transmission based on desired channel gain, that is, similar to the approach presented in [26]. In particular, the authors evaluate the achievable rate under different interference conditions. Results show that opportunistic transmission achieves a higher bit rate than random transmissions as well as the conventional non-opportunistic transmission.

By the above, it is clear that transmitting when the fading amplitude is above a threshold has been employed in different scenarios. Nevertheless, to our best knowledge, the performance of this transmission scheme has not been evaluated in encoded systems. On the other hand, other opportunistic approaches have been considered in the literature. For example, in [31], considering that it is easier for sensors to track large scale shadowing variations than small scale fading variations, the authors derive closed form expressions to evaluate the BER. The results show that opportunistic transmission, based on shadowing, can achieve very good performance improvements compared to typical transmissions. Thus, depending on the number of sensors in the network, the system has a gain in terms of SNR, but the diversity does not change. Moreover, in [32], the authors use opportunistic transmission for encoded cooperative networks, where the cooperation mode is activated based on outage events. In this work, 8-PSK modulation is employed to obtain some numerical results, where it is observed that the proposed scheme gains certain degrees of diversity compared to ordinary transmissions. Thus, the BER curves change their inclination but maintain a linear decayment when plotted as a function of the signal-to-noise ratio (SNR).

Considering that error correction codes are fundamental for adequate operation of wireless systems, in this work, an encoded opportunistic transmission scheme is evaluated in terms of the mean BER. Specifically, in the analyzed system, the encoded symbols are transmitted when the fading amplitude is above a threshold value. Because in specific scenarios, simulations can be time consuming, difficult to validate and does not present an explicit interdependence over all the system parameters, closed-form upper bound expressions to evaluate the mean BER are derived in this work considering convolutional and TCM codes. Nevertheless, the proposed transmission scheme can be employed with any kind of error correcting codes. To prove this, turbo codes [33] are also used in some simulations presented in this work. The above codes are considered because of their good performance and low implementation complexity, which make them to be used in many wireless standards. Consequently, the term opportunistic transmission is used quite profusely in the literature, but with quite different meanings. Thus, we affirm that in the literature there is no research on opportunistic transmission, as defined. Much less, combining opportunistic transmission with error correcting codes.

For the analysis, the channel considers presence of Rayleigh fading and additive white Gaussian noise (AWGN). Additionally, the presence of a time domain interleaving that

[1] In wireless systems, fading refers to a specific kind of attenuation which is highly frequency and time dependent.

TABLE 1. List of Symbols.

Symbol	Connotation
A	signal amplitude
B	bandwidth
$\mathbf{b}$	uncoded sequence of bits
$\mathbf{c}$	sequence of encoded symbols
$d^2_{\text{free,E}}$	Euclidean free distance
$d_{\text{free,H}}$	Hamming free distance
E_b	received energy per bit
f_c	carrier frequency
$f(x)$	probability density function of the random variable x
$\mathcal{G}$	coding gain
$g(t)$	Nyquist pulse format with duration T_s
$\mathbf{i}$	imaginary, $\mathbf{i} = \sqrt{-1}$
k	number of bits in an uncoded sequence
$\mathcal{L}$	transmitted sequence length
M	modulation order
n	number of encoded bits after the encoding process
N_0	unilateral noise power spectral density
p	non-transmission probability
$\overline{P_b}$	mean bit error rate
$\mathrm{P}(\cdot)$	probability operator
$\mathrm{P}(\mathbf{c} \to \mathbf{c}')$	pairwise error probability between $\mathbf{c}$ and $\mathbf{c}'$
q	transmission probability
r_c	encoder rate
R_b	bit rate
$\Re\{\cdot\}$	real operator
t	time
T_s	symbol duration
T_b	bit duration
$\mathcal{T}$	threshold value for the fading amplitude
α	Rayleigh fading amplitude
α_c	fading amplitude conditioned on $\alpha > \mathcal{T}$
$\overline{\gamma_c}$	mean signal-to-noise ratio
$\overline{\xi}$	mean spectral efficiency
$\mathbf{x}$	interleaved sequence of encoded symbols
σ	Rayleigh parameter
σ^2_n	noise variance

ensures independent fading on each symbol of the same encoded block is assumed. For more insightful analysis, the spectral efficiency and the coding gain are also analyzed. Simulations using the Monte Carlo method are carried out in order to verify the tightness of the derived expressions.

The remainder of this paper is organized as follows. The notation and the list of symbols is presented in Section II. The channel and system models are described in Section III. Some preliminary results related to opportunistic transmission are presented in Section IV. The system performance is analyzed in Section V. Numerical results and discussions are carried out in Section VI. Finally, the conclusions are presented in Section VII.

II. NOTATION AND LIST OF SYMBOLS

In what follows, lowercase letters, x, and bold lowercase letters, $\mathbf{x}$, denote scalars and vectors, respectively, and x_ℓ is the ℓ-th element of $\mathbf{x}$. Moreover, the connotation of each symbol employed along this paper is shown in Table 1.

III. CHANNEL AND SYSTEM DESCRIPTION

In this section, the channel model and the encoded opportunistic system are described.

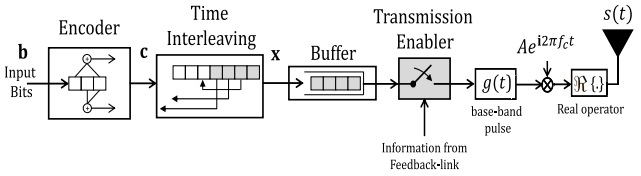

FIGURE 1. Encoded opportunistic transmitter block diagram.

A. CHANNEL DESCRIPTION

A flat-slow fading channel is considered. Let α be the random fading amplitude modeled as a Rayleigh random variable. Hence, its probability density function (PDF) is given by [40]

$$f(\alpha) = \frac{\alpha}{\sigma^2} \exp\left(-\frac{\alpha^2}{2\sigma^2}\right), \quad \alpha \geq 0, \tag{1}$$

where $2\sigma^2$ is the fading mean power. In addition, the received signals are also perturbed by AWGN. Consequently, the noise samples are modeled as zero-mean Gaussian random variables with variance

$$\sigma_n^2 = \frac{N_0}{4T_s}, \tag{2}$$

where N_0 is the unilateral noise power spectral density and T_s is the symbol duration.

B. TRANSMITTER AND RECEIVER DESCRIPTION

Fig. 1 shows the transmitter structure, where a sequence of binary digits with equal probability is generated. The bit sequence is denoted as $\mathbf{b} = (b_1, b_2, \ldots b_k)$. Afterwards, these bits are encoded. The sequence of complex encoded symbols is denoted by $\mathbf{c} = (c_1, c_2, \ldots c_L)$. These symbols belong to a constellation with normalized mean power. Then, this sequence passes through an ideal time interleaver, i.e., an interleaver with infinitely interleaving depth. This ensures that, after deinterleaving on the receiver side, the fading process is uncorrelated from symbol to symbol, which ensures some degrees of diversity [41]. The sequence of symbols at the interleaver output is denoted by $\mathbf{x} = (x_1, x_2, \ldots x_L)$. Finally, these symbols are stored into a buffer until the transmission is enabled. For this purpose, the receiver compares the instantaneous fading amplitude with a threshold value $\mathcal{T}$. If the fading amplitude is above $\mathcal{T}$, the receiver sends an enabler transmission command to the transmitter through a feedback link.[2] If the transmission is enabled, the symbols pass through a base-band pulse format filter, $g(t)$, that satisfies the Nyquist criterion. Then, the carrier is inserted. By the above, the sequence of encoded, interleaved and modulated transmitted symbols can be written as

$$s(t) = A\Re\left\{\sum_{\ell=1}^{\mathcal{L}} x_\ell\, g(t - \ell T_s) \exp(\mathbf{i}\, 2\pi f_c t)\right\}, \tag{3}$$

where t denotes time, A is the amplitude of the transmitted signal, $\mathcal{L}$ is the transmitted sequence length, x_ℓ is the ℓ-th

[2]The feedback link is considered as error-free.

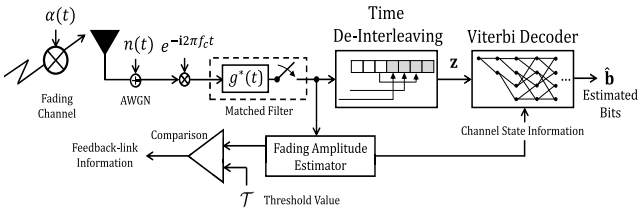

FIGURE 2. Encoded opportunistic receiver block diagram.

encoded and interleaved symbol, $g(t)$ is the Nyquist pulse format with unitary energy and f_c is the carrier frequency.

The received signal can be written as

$$r(t) = \alpha(t)s(t) + n(t), \tag{4}$$

where $\alpha(t)$ and $n(t)$ are independent stochastic processes. Specifically, $\alpha(t)$ and $n(t)$ are the fading amplitude and the noise as a function of time.

Fig. 2 shows the receiver structure, where the complex samples after the demodulation and deinterleaving processes are denoted by $\mathbf{z} = (z_1, z_2, ...z_L)$. Then, for convolutional and TCM codes, a Viterbi decoder performs maximum likelihood sequence estimation (MLSE) over these samples. MLSE criterion chooses the κ-th encoded sequence that minimizes the next cost function [43]:

$$\mathcal{M}_\kappa = \sum_{\ell=1}^{\mathcal{L}} \left| z_\ell - \alpha_\ell \, c_{\kappa,\ell} \right|^2, \tag{5}$$

where $c_{\kappa,\ell}$ denotes the ℓ-th symbol belonging to the κ-th possible encoded sequence. On the other hand, an iterative structure using a modified version of the classic maximum a-posteriory algorithm (MAP) [33] is invoked, in order to perform the decoding process when turbo codes are employed in the transmitter. Finally, at the decoder output, the sequence of estimated bits is $\hat{\mathbf{b}} = (\hat{b}_1, \hat{b}_2, ...\hat{b}_k)$.

A detailed explanation of convolutional, TCM and turbo encoders and decoders goes beyond the scope of this paper. The reader can refer to [41] and [42] for more information about their implementation in fading channels. However, it is important to indicate that for the opportunistic scheme, the decoder at the receiver requires channel state information (CSI), which is considered perfect in the following.

IV. OPPORTUNISTIC TRANSMISSION PRELIMINARIES

The opportunistic transmission scheme is presented in this section. A preliminary analysis is performed in order to provide BER expressions for uncoded systems. These expressions are also used in the following section.

The main idea behind opportunistic transmission is that users transmit only when the channel is in good condition, i.e., a user transmit when the fading amplitude is above a threshold $\mathcal{T}$. Fig. 3 compares ordinary (non-opportunistic) and opportunistic transmissions. Base-band symbols are considered for better understanding. In the figure, observe that ordinary transmission is performed despite the fading amplitude. On the other hand, opportunistic transmission is made only when the fading is above $\mathcal{T}$. As consequence, there are non-transmission periods. Let p be the probability that the instantaneous fading amplitude is below $\mathcal{T}$, i.e., p is the non-transmission probability. From (1), p can be obtained as a function of the threshold value as

$$\begin{aligned} p &= \int_0^{\mathcal{T}} \frac{\alpha}{\sigma^2} \exp\left(-\frac{\alpha^2}{2\sigma^2}\right) d\alpha \\ &= 1 - \exp\left(-\frac{\mathcal{T}^2}{2\sigma^2}\right). \end{aligned} \tag{6}$$

Consequently, the transmission probability, denoted as q, is

$$\begin{aligned} q &= 1-p \\ &= \exp\left(-\frac{\mathcal{T}^2}{2\sigma^2}\right). \end{aligned} \tag{7}$$

The Rayleigh fading conditioned on $\alpha > \mathcal{T}$ is denoted as α_c. From the results of [40, Section 4.4], the PDF of α_c is

$$f(\alpha_c) = \frac{\alpha_c}{\sigma^2} \exp\left(-\frac{\alpha_c^2 + \mathcal{T}^2}{2\sigma^2}\right), \quad \alpha_c > \mathcal{T}. \tag{8}$$

One way to counteract the non-transmission periods is by increasing the transmission rate, but this also increases the bandwidth required. Nevertheless, the transmission rate can be increased by increasing the modulation scheme. If the new modulation is selected appropriately, then the original bandwidth is not modified and the transmission rate of the ordinary system is maintained. For better understanding observe Fig. 3, where as example we can consider that the non-transmission probability is $p = 1/2$. Hence, an opportunistic system that modulates twice as many bits in each symbol as the ordinary system can be used in order to compensate for the transmission rate loss.

By the above, we can think that increasing the modulation will affect the system performance.[3] The question to answer in this case is: Will the opportunistic system, transmitting the same rate as an ordinary system, behave better or worse than that ordinary system?. In order to answer it, in the numerical results shown in Section VI, it is compared the performance of ordinary and opportunistic systems with the same transmission rate, translated in terms of the same spectral efficiency.

A. MEAN BIT ERROR RATE

In uncoded scenarios, the mean bit error rate (BER) of a user employing opportunistic transmission can be obtained as

$$\overline{P_b} = \int_{\mathcal{T}}^{\infty} P(b|\alpha_c) f(\alpha_c) d\alpha_c, \tag{9}$$

where $P(b|\alpha_c)$ denotes the BER conditioned on the instantaneous fading amplitude.

In the following, BER expressions for BPSK and M-QAM modulations are derived.

[3] A greater modulation order implies higher transmission rate but the system is more susceptible to the channel effects.

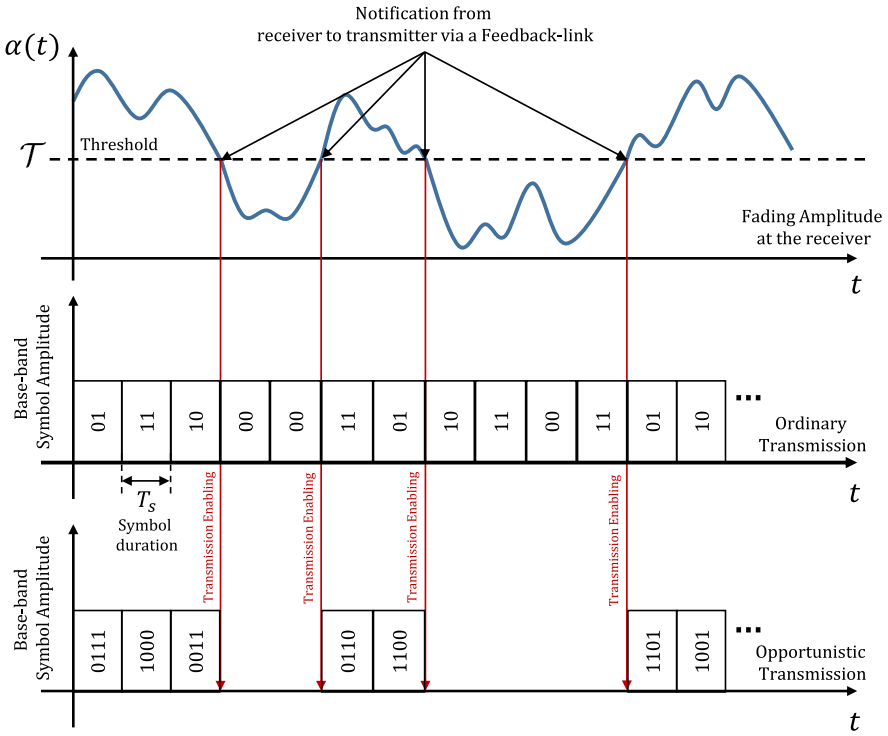

FIGURE 3. Opportunistic transmission.

1) BPSK MODULATION

In this scenario, the BER conditioned on the instantaneous fading amplitude is [43]

$$P(b|\alpha_c) = \frac{1}{2}\,\mathrm{erfc}\left(\sqrt{\alpha_c^2 \frac{E_b}{N_0}}\right), \tag{10}$$

where $\mathrm{erfc}(x)$ is the complementary error function, defined as [40]

$$\mathrm{erfc}(x) = \frac{2}{\sqrt{\pi}} \int_x^\infty \exp(-y^2) dy, \tag{11}$$

and E_b is the received energy per bit.

Before calculate the mean BER for BPSK modulation, we define the mean SNR per received symbol, $\overline{\gamma_c}$, as

$$\overline{\gamma_c} = 2\sigma^2 \frac{E_b}{N_0} \log_2 M, \tag{12}$$

where $2\sigma^2$ is the Rayleigh fading mean power and M is the modulation order. For BPSK, $M = 2$. In this case $\overline{\gamma_c} = 2\sigma^2 E_b/N_0$ represents the mean SNR per received bit.

By employing (7)-(12), Appendix A shows that the mean BER for BPSK modulation is given by

$$\overline{P_b} = \frac{\sigma^2}{q}\left[\mathrm{erf}\left(\mathcal{T}\sqrt{\frac{1+\overline{\gamma_c}}{2\sigma^2}}\right) - 1\right]\left(1 + \frac{1}{\overline{\gamma_c}}\right)^{-\frac{1}{2}} + \sigma^2\,\mathrm{erfc}\left(\mathcal{T}\sqrt{\frac{\overline{\gamma_c}}{2\sigma^2}}\right), \tag{13}$$

where $\mathrm{erf}(x)$ denotes the error function and it is obtained as $\mathrm{erf}(x) = 1 - \mathrm{erfc}(x)$.

Appendix B shows that for large x, (11) can be approximated by

$$\mathrm{erfc}(x) \approx \frac{1}{x\sqrt{\pi}} \exp\left(-x^2\right). \tag{14}$$

With the above result, in the high SNR regime, (13) can be approximated by

$$\overline{P_b} \approx \frac{1}{2}\,\mathrm{erfc}\left(\mathcal{T}\sqrt{\frac{\overline{\gamma_c}}{2\sigma^2}}\right)\left(\frac{1}{2\sigma^2} + \overline{\gamma_c}\right)^{-1}. \tag{15}$$

By comparing (10) with (15), note that the mean SNR appears within the $\mathrm{erfc}(\cdot)$ function in both expressions. As consequence of that, they have a similar behavior. It means that BER curves for opportunistic transmission, when plotted as a function of the mean SNR, have a exponential decayment.[4] This suggests that opportunistic transmission strongly mitigates the fading effects. This is verified in the numerical results performed in Section VI.

2) M-QAM MODULATION

Considering Gray encoding, the BER conditioned on the instantaneous fading amplitude for square M-QAM

[4]The exponential decayment comes from the $\mathrm{erfc}(\cdot)$ function behavior. Note that its approximation, given by (14), has an exponential form.

modulations is [43]

$$P(b|\alpha_c) = \frac{2(\sqrt{M}-1)}{\sqrt{M}\log_2 M}\,\text{erfc}\left(\sqrt{\frac{\alpha_c^2}{\zeta}\frac{E_b}{N_0}\log_2 M}\right), \quad (16)$$

where $\zeta = 2(M-1)/3$. From (7)-(9), (12) and (16), the mean BER for opportunistic transmission with M-QAM modulations is given by

$$\overline{P_b} = \frac{2(\sqrt{M}-1)}{\sqrt{M}\log_2 M}\left\{\frac{2\sigma^2}{q}\left(1+\frac{\zeta}{\overline{\gamma_c}}\right)^{-\frac{1}{2}} \times\left[\text{erf}\left(\mathcal{T}\sqrt{\frac{1+\overline{\gamma_c}/\zeta}{2\sigma^2}}\right)-1\right]+\text{erfc}\left(\mathcal{T}\sqrt{\frac{\overline{\gamma_c}}{2\sigma^2\zeta}}\right)\right\}. \quad (17)$$

Employing (14), (17) can be approximated by

$$\overline{P_b} \approx \frac{(\sqrt{M}-1)}{\sqrt{M}\log_2 M}\left(\frac{2\sigma^2}{1+\overline{\gamma_c}/\zeta}\right)\text{erfc}\left(\mathcal{T}\sqrt{\frac{\overline{\gamma_c}}{2\sigma^2\zeta}}\right). \quad (18)$$

B. SPECTRAL EFFICIENCY

The spectral efficiency is defined as the bit rate, R_b, that can be transmitted over a given bandwidth, B. With the opportunistic scheme, transmissions occur with probability q. Consequently, the bit rate is equal to $R_b = q\log_2 M/T_s$ bits/s. As the bandwidth is equal to $B = 1/T_s$ Hz, the mean spectral efficiency is equal to

$$\overline{\xi} = \frac{R_b}{B} = q\log_2 M \quad \text{bits/s/Hz}. \quad (19)$$

As particular case, if $q = 1$, then (19) becomes the spectral efficiency of an ordinary system, i.e., a system that transmits all the time regardless the fading amplitude.

By the above, the non-transmission periods represent loss of spectral efficiency. Nevertheless, it is possible to compensate for this loss by increasing the modulation order. Specifically, the modulation order can be expanded from M to $M^{\frac{1}{q}}$, similar to what is done with TCM codes.

V. PERFORMANCE ANALYSIS

Expressions to evaluate the mean BER for encoded opportunistic transmission are obtained in this section. Convolutional and TCM codes are considered.

A. CONVOLUTIONAL CODES SCENARIO

In convolutional codes, codewords are generated employing linear operations into a finite state machine. In general, a convolutional code is represented as (n, k, m), where n is the number of encoded bits, k is the number of message bits and m is the total number of memories employed by the encoder. Generally, n and k are small integers satisfying that $k < n$. Moreover, as larger is m, better is the system performance and higher is the decoding complexity [11]. The ratio between the number of message bits and the number of encoded bits is known as encoder rate $r_c = k/n$. A convolutional encoder can be represented by a generator matrix, which produces a state diagram or a trellis [13].

1) MEAN BIT ERROR RATE

Convolutional codes performance in AWGN channel is determined by r_c and by the Hamming free distance, which is defined as [13]

$$d_{\text{free,H}} \triangleq \min\left\{d(\mathbf{c},\mathbf{c}') : \mathbf{b} \neq \mathbf{b}'\right\}, \quad (20)$$

where $\mathbf{c}$ and $\mathbf{c}'$ are encoded sequences obtained from the information sequences $\mathbf{b}$ and $\mathbf{b}'$, respectively. In addition, $d(\mathbf{c},\mathbf{c}')$ denotes the Hamming distance between $\mathbf{c}$ and $\mathbf{c}'$. The greater $d_{\text{free,H}}$, the greater the minimum separation between encoded sequences. Consequently, the greater is the correction capability in the decoding process.

For linear codes, it is possible to assume that the all-zero sequence is transmitted. In this case, the BER is related to the probability that the detector chooses another sequence different of the all-zero sequence. Under this assumption, the mean BER upper bound for convolutional codes in AWGN channel is obtained as [44]

$$\overline{P_b} < \frac{1}{k}\sum_{d=d_{\text{free,H}}}^{\infty}\mathcal{B}_d\mathcal{R}_d, \quad (21)$$

with $\mathcal{B}_d = \mathcal{A}_d\mathcal{N}_d$, where $\mathcal{A}_d$ is the number of paths with Hamming distance d from the all-zero sequence and $\mathcal{N}_d$ is the number of information bits in error in that path. Moreover, $\mathcal{R}_d$ is given by [13]

$$\mathcal{R}_d = P_{\text{f}}^d\sum_{\ell=0}^{d-1}\binom{d-1+\ell}{\ell}(1-P_{\text{f}})^{\ell}, \quad (22)$$

where P_{f} is the mean BER in fading channels. Considering that the encoded bits are modulated employing BPSK modulation, P_{f} is calculated as [43]

$$P_{\text{f}} = \frac{1}{2}\left(1-\sqrt{\frac{r_c\overline{\gamma_c}}{1+r_c\overline{\gamma_c}}}\right), \quad (23)$$

where $\overline{\gamma_c}$ is given by (12). Finally, it is important to indicate that (21) is calculated considering all possible encoded sequences, which are compared with the all-zero sequence.

For $r_c\overline{\gamma_c} \gg 1$, $P_{\text{f}} \approx (4\,r_c\overline{\gamma_c})^{-1}$ and thus, $P_{\text{f}} \ll 1$. As consequence, $\mathcal{R}_d \approx P_{\text{f}}^d\binom{2d-1}{d}$. In addition, the first term in the summation of (21) is dominant. Therefore, an upper bound for (21) is calculated as

$$\overline{P_b} \approx \frac{1}{k}\mathcal{B}_{d_{\text{free,H}}}\binom{2d_{\text{free,H}}-1}{d_{\text{free,H}}}\left(\frac{1}{4r_c\overline{\gamma_c}}\right)^{d_{\text{free,H}}}. \quad (24)$$

From (24), $\overline{P_b} \propto \gamma_c^{-d_{\text{free,H}}}$. Hence, a system employing convolutional codes in a fading channel has diversity $d_{\text{free,H}}$.

Now, the mean BER for convolutional encode opportunistic transmission is calculated. For this scenario, the mean BER upper bound can be easily obtained from the results of Section IV and the result of (21). As this expression is a function of the BER in fading channels, P_{f}, can be replaced

by (13) but considering also the encoding rate. Hence, the new P_{f} to be employed in (22), named as $P_{\mathrm{f,o}}$, is given by

$$P_{\mathrm{f,o}} = \frac{\sigma^2}{q}\left[\operatorname{erf}\left(\mathcal{T}\sqrt{\frac{1+r_c\overline{\gamma_c}}{2\sigma^2}}\right)-1\right]\left(1+\frac{1}{r_c\overline{\gamma_c}}\right)^{-\frac{1}{2}} + \sigma^2 \operatorname{erfc}\left(\mathcal{T}\sqrt{\frac{r_c\overline{\gamma_c}}{2\sigma^2}}\right). \tag{25}$$

Consequently, the mean BER upper bound for convolutional encoded opportunistic transmission is obtained replacing (25) in (22) and then, this result in (21). Considering the results of (15) and (24), this mean BER upper bound can be approximated by

$$\overline{P_b} \approx \frac{1}{k}\mathcal{B}_{d_{\mathrm{free,H}}}\binom{2d_{\mathrm{free,H}}-1}{d_{\mathrm{free,H}}}\left[\frac{1}{2}\operatorname{erfc}\left(\mathcal{T}\sqrt{\frac{r_c\overline{\gamma_c}}{2\sigma^2}}\right)\right]^{d_{\mathrm{free,H}}} \times\left(\frac{1}{2\sigma^2}+r_c\overline{\gamma_c}\right)^{-d_{\mathrm{free,H}}}. \tag{26}$$

In the above expression, the factor in brackets is the one that decreases more rapidly as $\overline{\gamma_c}$ increases. Therefore, this factor defines the BER curve behavior. Thus, from (14) and (26), the BER for convolutional encoded opportunistic transmission has an exponential decayment as $\overline{\gamma_c}$ increases.

2) CODING GAIN

The coding gain is defined as the ratio between the SNR required by uncoded and encoded systems in order to reach the same BER in the asymptotic region. For convolutional codes in AWGN channel, the coding gain is given approximately by the product of the coding rate and the Hamming free distance [13], that is

$$\mathcal{G} \approx r_c d_{\mathrm{free,H}}. \tag{27}$$

Even though this expression is valid for AWGN channels, the numerical results of Section VI show that (27) can also be used for scenarios with opportunistic transmission. This is due to the exponential decayment of the BER curves when they are plotted as a function of the SNR.

3) SPECTRAL EFFICIENCY

For this scenario, the bit rate is $R_b = 1/T_b$ bits/s, where it is considered that the bit duration is equal to the symbol duration, i.e., $T_b = T_s$. The minimum Nyquist bandwidth is given by $B = 1/(r_c T_b)$ Hz. As a consequence, the mean spectral efficiency is

$$\overline{\xi} = \frac{R_b}{B} = r_c \quad \text{bits/s/Hz}. \tag{28}$$

Hence, convolutional codes expand the bandwidth. Moreover, convolutional encoded opportunistic transmission provides a bit rate equal to $R_b = q/T_b$ bits/s. The minimum Nyquist bandwidth is given by $B = 1/(r_c T_b)$ Hz. Therefore, the mean spectral efficiency for this scenario is given by

$$\overline{\xi} = \frac{R_b}{B} = q r_c \quad \text{bits/s/Hz}. \tag{29}$$

B. TRELLIS CODED MODULATION SCENARIO

TCM allows noise immunity without altering the employed bandwidth. With this aim, the modulation order is expanding from 2^k to $M' = 2^n$. A TCM encoder is comprised of a convolutional encoder with rate $r_c = k/n$ followed by a modulator whose constellation contains $M' = 2^n$ symbols.

1) MEAN BIT ERROR RATE

The TCM performance is measured in terms of the minimum squared Euclidean distance (MSED). The MSED between the sequences $\mathbf{c}$ and $\mathbf{c}'$ is calculated employing

$$d^2_{\mathrm{free,E}} = \min_{\mathbf{c}\neq\mathbf{c}'\in\mathcal{C}}\sum_{j\in\eta}\left|c_j - c'_j\right|^2, \tag{30}$$

where $\mathcal{C}$ is the set of all encoded sequences and η is the set of positions where the encoded symbol sequences $\mathbf{c}$ and $\hat{\mathbf{c}}$ are different.

In order to derive an upper bound for the mean BER of a system employing TCM in fading channels, the pairwise error probability concept [45] can be employed. Thus, this mean BER upper bound is obtained as

$$\overline{P_b} \leq \sum_{\mathbf{c}\in\mathcal{C}}\sum_{\mathbf{c}'\in\mathcal{C}}\beta(\mathbf{c},\mathbf{c}')\mathrm{P}(\mathbf{c})\mathrm{P}(\mathbf{c}\to\mathbf{c}'), \tag{31}$$

where $\beta(\mathbf{c},\mathbf{c}')$ is the number of bits in error appearing when the sequence $\mathbf{c}$ is transmitted and the sequence $\mathbf{c}' \neq \mathbf{c}$ is chosen by the decoder, $\mathrm{P}(\mathbf{c})$ is the a priori probability of transmitting $\mathbf{c}$ and $\mathrm{P}(\mathbf{c}\to\mathbf{c}')$ is the pairwise error probability, that is, the probability that the decoder chooses $\mathbf{c}'$ when indeed $\mathbf{c}$ was transmitted. Note that (31) is calculated for all $\mathbf{c},\mathbf{c}' \in \mathcal{C}$.

The pairwise error probability conditioned on the instantaneous fading amplitudes is given by [34]

$$\mathrm{P}(\mathbf{c}\to\mathbf{c}'|\alpha_j) \leq \exp\left[-\frac{1}{4}\overline{\gamma_c}\, d^2(\mathbf{c},\mathbf{c}')\right], \tag{32}$$

where

$$d^2(\mathbf{c},\mathbf{c}') \triangleq \sum_{j\in\eta}\alpha_j^2\left|c_j - c'_j\right|^2 \tag{33}$$

represents the square of the Euclidean distance between the symbol sequences $\mathbf{c}$ and $\mathbf{c}'$, η is the set of all j for which $c_j \neq c'_j$ and α_j is the fading amplitude on the j-th time interval whose PDF is given by (1). Considering ideal time interleaving, the random variables α_j are independent and identically distributed (i.i.d) for all j. Thus, the upper bound for the pairwise error probability can be obtained by averaging (32). Hence, we have that

$$\mathrm{P}(\mathbf{c}\to\mathbf{c}') \leq \int_0^\infty \cdots \int_0^\infty \mathrm{P}(\mathbf{c}\to\mathbf{c}'|\alpha_j)\prod_{j\in\eta} f(\alpha_j)d\alpha_j. \tag{34}$$

Solving (34), the upper bound of the pairwise error probability is given by

$$\mathrm{P}(\mathbf{c}\to\mathbf{c}') \leq \left(\prod_{j\in\eta}\frac{1}{4}\overline{\gamma_c}\left|c_j - c'_j\right|^2\right)^{-1}. \tag{35}$$

Finally, substituting (35) in (31), we get the upper bound of the mean BER for TCM codes, that can be written as

$$\overline{P_b} \leq \sum_{\mathbf{c}\in\mathcal{C}} \sum_{\mathbf{c}'\in\mathcal{C}} \beta(\mathbf{c},\mathbf{c}')\mathrm{P}(\mathbf{c}) \left(\prod_{j\in\eta} \frac{1}{4}\overline{\gamma_c} \left| c_j - c_j' \right|^2 \right)^{-1}. \quad (36)$$

In order to derive an upper bound for the mean BER of TCM encoded opportunistic transmission we rewrite (34) as

$$\begin{aligned} \mathrm{P}(\mathbf{c}\to\mathbf{c}') &\leq \int_{\mathcal{T}}^{\infty} \cdots \int_{\mathcal{T}}^{\infty} \mathrm{P}(\mathbf{c}\to\mathbf{c}'|\alpha_{c,j}) \prod_{j\in\eta} f(\alpha_{c,j}) d\alpha_{c,j} \\ &\leq \int_{\mathcal{T}}^{\infty} \cdots \int_{\mathcal{T}}^{\infty} \exp\left(-\frac{1}{4}\overline{\gamma_c} \sum_{j\in\eta} \alpha_{c,j}^2 \left| c_j - c_j' \right|^2 \right) \\ &\quad \times \prod_{j\in\eta} f(\alpha_{c,j}) d\alpha_{c,j}, \end{aligned} \quad (37)$$

where $f(\alpha_{c,j})$ is given by (8) and we have employed the results of (32) and (33). Because $\alpha_{c,j}$ are i.i.d. random variables $\forall j$, (37) has a closed-form given by

$$\mathrm{P}(\mathbf{c}\to\mathbf{c}') \leq \prod_{j\in\eta} \frac{1}{q^j} \frac{\exp\left[-\frac{\mathcal{T}^2}{\sigma^2} \left(1 + \frac{1}{4}\overline{\gamma_c} \left| c_j - c_j' \right|^2 \right) \right]}{1 + \frac{1}{4}\overline{\gamma_c} \left| c_j - c_j' \right|^2}. \quad (38)$$

Substituting (38) in (31), we get the upper bound for the mean BER of TCM encoded opportunistic transmission, that is written as

$$\begin{aligned} \overline{P_b} \leq & \sum_{\mathbf{c}\in\mathcal{C}} \sum_{\mathbf{c}'\in\mathcal{C}} \beta(\mathbf{c},\mathbf{c}')\mathrm{P}(\mathbf{c}) \\ & \times \prod_{j\in\eta} \frac{1}{q^j} \frac{\exp\left[-\frac{\mathcal{T}^2}{\sigma^2} \left(1 + \frac{1}{4}\overline{\gamma_c} \left| c_j - c_j' \right|^2 \right) \right]}{1 + \frac{1}{4}\overline{\gamma_c} \left| c_j - c_j' \right|^2}. \end{aligned} \quad (39)$$

Note that (39) depends on the Euclidean distance between the symbols of two different encoded sequences. The M-ary trellis of the code can be used to calculate these distances.

2) CODING GAIN

The coding gain is given approximately by the ratio between the squared Euclidean free distance ($d^2_{\text{free,E}}$) of the expanded constellation and the minimum square distance of the original constellation [34], that is

$$\mathcal{G} \approx \frac{d^2_{\text{free,E}}}{d^2_{\min}}. \quad (40)$$

3) SPECTRAL EFFICIENCY

The bit rate employing TCM codes is $R_b = \frac{1}{T_s}\log_2 M$ bits/s, where $M = 2^k$. The minimum Nyquist bandwidth is $B = 1/T_s$ Hz. As a consequence the mean spectral efficiency is

$$\overline{\xi} = \frac{R_b}{B} = \log_2 M \quad \text{bits/s/Hz}. \quad (41)$$

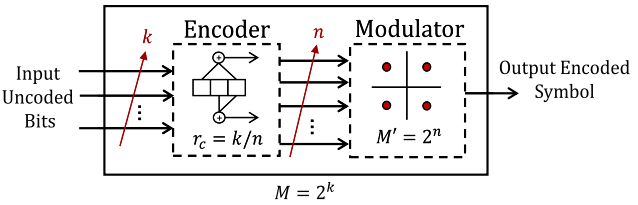

FIGURE 4. TCM encoder structure.

Therefore, TCM does not expand the bandwidth. For better understanding observe Fig. 4.

Finally, TCM encoded opportunistic transmission provides a bit rate equal to $R_b = \frac{q}{T_s}\log_2 M$ bits/s and the minimum Nyquist bandwidth is given by $B = 1/T_s$ Hz. Hence, the mean spectral efficiency is given by

$$\overline{\xi} = \frac{R_b}{B} = q\log_2 M \quad \text{bits/s/Hz}, \quad (42)$$

which expands the bandwidth, except if the modulation order employed is equal to $M^{\frac{1}{q}}$.

C. TURBO CODES SCENARIO

In the transmitter, turbo codes are generated employing a parallel concatenation of two recursive systematic convolutional (RSC) codes, with an interleaver between the two encoders. At the receiver, the iterative MAP is used in order to perform the decoding process. In particular, MAP algorithm provides not only the estimated bit sequence, but also the probabilities for each bit that it has been decoded correctly. This is essential for the iterative decoding of turbo codes [35].

Finding expressions to evaluate the BER of systems employing turbo codes can become quite intricate. For this reason, several works have evaluated their BER based on simulations [36]–[39]. Moreover, in the literature, it is known that the number of iterations performed in the MAP detector directly affects the system performance. In this sense, the performance of opportunistic transmission with turbo codes is evaluated as a function of the number of iterations via simulations in Section VI.

VI. NUMERICAL RESULTS

In this section, we assess the performance of the proposed scheme in some representative scenarios. Simulations employing the Monte Carlo method are carried out in order to verify the accuracy of the derived expressions.

The simulations have been performed employing the error correcting codes detailed on Table 2. In addition, the fading mean power has been normalized, i.e., $2\sigma^2 = 1$.

Fig. 5 shows the mean BER as a function of E_b/N_0 for uncoded and encoded ordinary systems (non-opportunistic) and for uncoded and encoded opportunistic systems with BPSK modulation. Encoded scenarios use the code C_1 of Table 2. The Hamming free distance for this code is $d_{\text{free,H}} = 5$. For opportunistic transmission scenarios, the transmission probability is set to $q = 1/2$. Note the accuracy between theoretical and simulation results. In particular, BER curves for ordinary transmissions are

TABLE 2. Employed Error Correcting Codes.

Identifier	Code Generator	r_c	m_t	Type	Modulation
C_1	[5 7]	1/2	2	Convolut.	BPSK
C_2	[5 2]	1/2	2	TCM	QPSK
C_3	[33 14 5 10]	1/4	4	TCM	16-QAM
C_4	[11 2 4 10]	3/4	3	TCM	16-QAM
C_5	[7; 5]	1/2	2	Turbo	BPSK

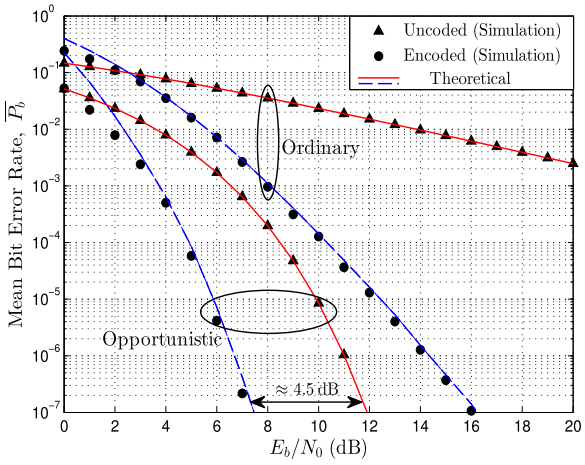

FIGURE 5. Mean BER as a function of E_b/N_0 for different scenarios considering BPSK modulation. Encoded scenarios employ convolutional encoding via the code C_1. Opportunistic transmission is applied with $q = 1/2$.

obtained employing $\mathcal{T} = 0$, or equivalently, $q = 1$. Moreover, some curves are accurate only in the low BER region because they are upper bounds. Note that the BER curve for the uncoded non-opportunistic scenario has a linear decayment as E_b/N_0 increases. In particular, in the literature it is known that the diversity is equal to 1 for this scenario [43]. On the other hand, note that the BER curve for the opportunistic system has an exponential decayment as E_b/N_0 increases. This can be verified in the BER expression given by (13) and with more detail in its approximation, given by (14), where the erfc(·) function has the exponential behavior. This can be verified in its approximate expression, which is given by (15). Therefore, opportunistic transmission presents the best performance. Obviously, encoded systems have better performance than uncoded ones. Compare uncoded with encoded opportunistic results in the low BER region. Notice that the second scenario requires approximately 4.5 dB less E_b/N_0 in order to guarantee the same BER than the first scenario. The expected coding gain, given by (27), is approximately 4 dB. This shows that the aforementioned expression can also be used for opportunistic transmission scenarios due to the BER curves behavior. As a particular case, the uncoded scenarios have a slightly lower BER than the encoded ones in the low E_b/N_0 region. To explain this behavior, it is important to indicate that to make a fair comparison, the encoded and uncoded systems must guarantee the same transmission power for each uncoded bit. Thus,

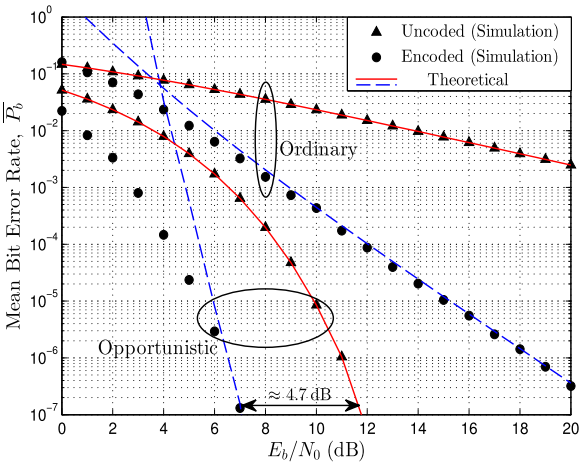

FIGURE 6. Mean BER as a function of E_b/N_0 for different scenarios considering QPSK modulation. Encoded scenarios employ TCM encoding via the code C_2. Opportunistic transmission is applied with $q = 1/2$.

the encoded systems transmit a lower power per bit (encoded or uncoded). As a result, it is observed that the encoded systems have a performance slightly lower than that of the uncoded systems in the region of very low E_b/N_0. Specifically, the code has not yet started to work properly in this region. However, this is a particular case, as this may change depending on the type of code used. Thus, more powerful codes may not present this type of behavior when compared to uncoded systems. Finally, another interesting scenario to note is that uncoded opportunistic system has better performance than encoded ordinary systems. It is relevant to state that both systems have the same mean spectral efficiency of $\overline{\xi} = 1/2$ bits/s/Hz. In addition, uncoded opportunistic systems are superior to encoded ordinary systems not only in performance but they also have smaller complexity implementation.

Fig. 6 is similar to the previous figure, but in this case 4-QAM modulation (QPSK) is used. The encoded systems employ TCM with the code C_2 of Table 2 and the opportunistic transmission applies $q = 1/2$. For the code employed, $d^2_{\text{free,E}} = 10$ and for QPSK modulation, $d^2_{\min} = 4$. Hence, from (40), the expected coding gain is $\mathcal{G} \approx 4$ dB. In the figure, note that encoded opportunistic system requires approximately 4.7 dB less E_b/N_0 in order to guarantee the same BER than uncoded opportunistic system. Moreover, notice that uncoded opportunistic system has better performance than encoded ordinary one although both systems have the same spectral efficiency, which is $\overline{\xi} = 1$ bits/s/Hz. In a similar way to what was observed in Fig. 5, notice in Fig. 6 that the BER curves for the opportunistic case present exponential decayment as E_b/N_0 increases. It is also verified in (15), (18), (26) and (39). In particular, the erfc(·) function has an exponential decayment in these expressions. This behavior is not observed in other opportunistic transmission approaches [31], [32], where the systems gains some degrees of diversity, but the BER curves maintain a linear decayment when E_b/N_0 increases. Hence, these schemes may

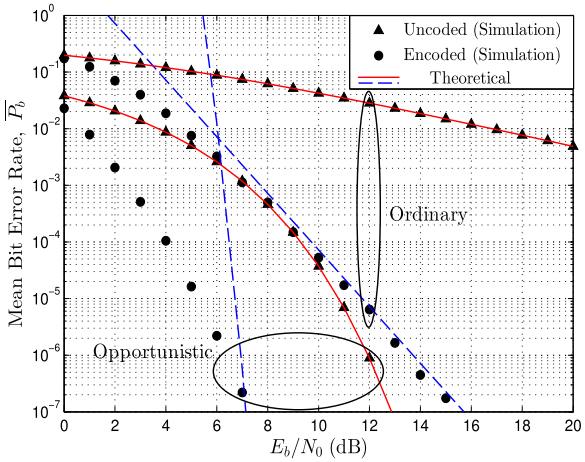

FIGURE 7. Mean BER as a function of E_b/N_0 for different scenarios considering 16-QAM modulation. Encoded scenarios employ TCM encoding via the code C_3. Opportunistic transmission is applied with $q = 1/4$.

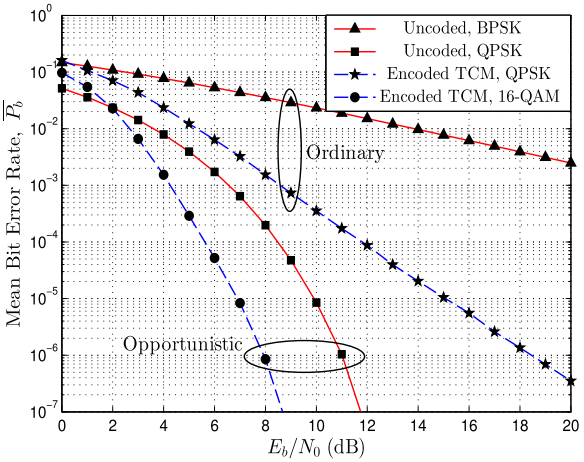

FIGURE 8. Mean BER as a function of E_b/N_0 for different scenarios with spectral efficiency $\overline{\xi} = 1$ bits/s/Hz.

require a greater E_b/N_0 to guarantee the same BER than our proposal.

Fig. 7 shows the mean BER as a function of the E_b/N_0 ratio for uncoded and encoded ordinary systems and for uncoded and encoded opportunistic systems employing 16-QAM modulation. The encoded scenarios use TCM with the code C_3 of Table 2. The opportunistic transmission applies a transmission probability $q = 1/4$. Note that theoretical curves are accurate with simulation results. Even when q and r_c decrease, the uncoded opportunistic system maintains better performance than the encoded ordinary system. While the mean BER curve of the uncoded opportunistic system decays exponentially, the mean BER curve of the encoded ordinary system decays linearly. Notice that both systems present the same spectral efficiency of $\overline{\xi} = 1$ bits/s/Hz. Finally, observe that the encoded opportunistic system has the best performance. However, the mean spectral efficiency for this scenario is $\overline{\xi} = 1/4$ bits/s/Hz.

In order to make a fair comparison, systems with the same spectral efficiency are considered in Fig. 8, which compares the BER curves obtained for different scenarios with spectral efficiency $\overline{\xi} = 1$ bits/s/Hz. The systems considered are uncoded ordinary with BPSK modulation, uncoded opportunistic employing QPSK modulation and $q = 1/2$, encoded TCM ordinary employing the code C_2 with QPSK modulation and encoded TCM opportunistic employing the code C_4, 16-QAM modulation and $q = 1/3$. For simplicity, only simulation results have been plotted. The fact that all systems have the same spectral efficiency implies that the ratio between the transmitted bit rate and the used bandwidth is maintained in all scenarios. Although the proposed opportunistic scheme enables transmission only when the fading amplitude is above a threshold value, the transmitted bit rate may be maintained by increasing the modulation order, which ensures that the bandwidth is not increased. In the results, note that the encoded opportunistic scenario presents the best performance. Observe also that the uncoded opportunistic

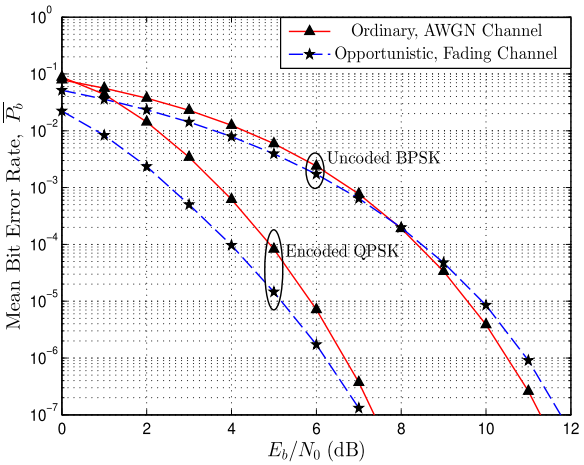

FIGURE 9. Mean BER as a function of E_b/N_0 in AWGN and fading channels for uncoded and encoded ordinary and opportunistic transmissions.

system has better performance than both ordinary systems. Therefore, from a performance viewpoint, the encoded opportunistic system can be considered as the best option. However, considering the complexity-performance trade-off, the uncoded opportunistic approach is an interesting option because it requires only 3.5 dB more E_b/N_0 than the encoded opportunistic system in order to guarantee the same BER, but with lower implementation complexity.

The derived BER expressions and the above numerical results show the exponential behavior of the BER curves for opportunistic systems when they are plotted as a function of E_b/N_0. This behavior occurs for both uncoded and encoded systems operating in fading channels. This shows that the fading effects are strongly attenuated. Consequently, opportunistic systems in fading channels exhibit similar performance to ordinary systems that operate in AWGN channels. To corroborate this, Fig. 9 shows the following scenarios: uncoded ordinary system in AWGN channel employing BPSK modulation, encoded TCM ordinary system in AWGN channel employing

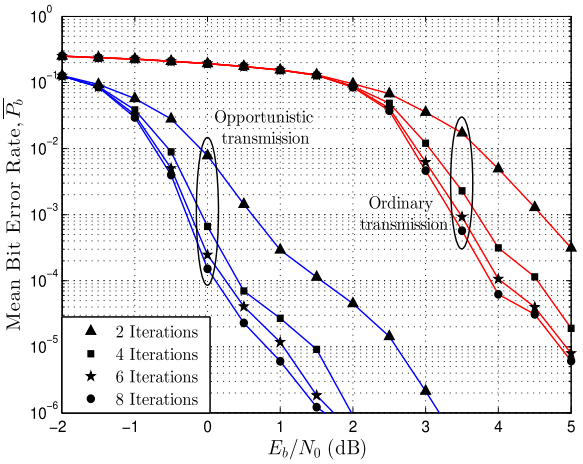

FIGURE 10. Mean BER as a function of E_b/N_0 for turbo encoded systems, via the code C_5, employing ordinary and opportunistic transmissions, with $q = 1/2$, and parameterized by the number of iterations performed by MAP.

the code C_2, uncoded opportunistic system in a Rayleigh fading channel employing BPSK modulation with $q = 1/2$ and encoded TCM opportunistic system in Rayleigh fading channel employing the code C_2 and $q = 1/2$. Notice the exponential behavior of all the BER curves. As result of this similarity, a comparable coding gain is observed for AWGN and fading scenarios. For the chosen code, it is obtained $d^2_{\text{free,E}} = 10$ and for QPSK the minimum square distance is $d^2_{\text{min}} = 4$. Hence, from (40), the coding gain is $\mathcal{G} \approx 4.0$ dB. In the figure, it is expected that at one point the BER curve of the encoded ordinary system in AWGN and the BER curve of the opportunistic encoding system in fading channel intersect and thus, the first system will be better, similar to what is observed in the uncoded scenario.

Finally, in order to show that the proposed scheme can be used with other types of error correcting codes, Fig. 10 shows the mean BER as a function of E_b/N_0 for turbo encoded systems. In this figure, the code C_5 of Table 2 was used for ordinary and opportunistic transmissions parameterized by the number of iterations performed by the MAP detector. As stated earlier, it is not straightforward to obtain theoretical results for turbo codes because of the iterative nature of the detector. For this reason, only simulations are presented in the figure. In the results, note again the advantages of the opportunistic transmission scheme, since it is possible to obtain a lower BER even with a lower complexity, that is, with a lower number of iterations in the detector, the opportunistic transmission ensures a lower BER than the ordinary transmission. The behavior of the BER curves of this type of codes, when they are plotted as a function of the E_b/N_0 is quite particular. Thus, it is not observed that the curves change their diversity, or equivalently their slope when the E_b/N_0 increases, as happens with convolutional or TCM codes in ordinary transmissions. Rather, with turbo codes, the BER curves decay rapidly as E_b/N_0 increases. Nevertheless, it is interesting to observe that with opportunistic transmission, the decayment of the BER curves seems similar to that of the ordinary scenario but with a significant gain in terms of E_b/N_0 and how it was indicated, this implies that fewer iterations can be performed in the MAP detector.

VII. CONCLUSION

In this paper, a transmission scheme combining error correcting codes with opportunistic transmission is proposed. The main idea behind this scheme is that encoded symbols are transmitted only when the fading amplitude is above a threshold. The performance of this scheme is analyzed in terms of the mean BER. Closed-form upper bound expressions were derived for convolutional and TCM codes. The expressions are very tight and they are in total concordance with the simulation results. Moreover, turbo codes were also employed in some simulations. In this case, it was observed that opportunistic transmission can highly reduce the detector complexity since a lower BER can be obtained performing fewer iterations in the MAP detector than in the ordinary transmission scenario.

Results showed that uncoded and encoded opportunistic systems are superior to uncoded and encoded ordinary ones. In addition, it was observed that uncoded opportunistic systems are superior to encoded ordinary systems. These results were obtained by guaranteeing the same spectral efficiency for all the systems. It is relevant to state that the implementation of opportunistic systems is much less complex than encoded ordinary systems. In addition, the rapid decayment of the BER curves suggests that fading effects are highly attenuated. Moreover, for convolutional and TCM codes, it is observed that the coding gain of encoded opportunistic systems over uncoded opportunistic systems in fading channel is similar to the coding gain of encoded ordinary systems over uncoded ordinary systems in AWGN channel.

At this point, some future research proposals in addition to the work developed are provided. In this work, it has been considered an error-free feedback link. However, depending on how the feedback link is transmitted if via Time Division Duplex (TDD), or Frequency Division Duplex (FDD), opportunistic transmission may be more or less susceptible to the undesired effects of fading in the feedback channel. In addition, another aspect to be analyzed is that channels may vary rapidly, so feedback channels can have some difficulties. Therefore, to look for mechanisms that allow opportunistic transmission to be used in these type of channels is desirable. Finally, while most current cellular systems use turbo codes, the trend for new cellular systems is to use the the so-called polar codes [22]. Thus, another future work would consists of evaluating the performance of opportunistic systems using this type of coding.

APPENDIX A
OPPORTUNISTIC TRANSMISSION MEAN BER EMPLOYING BPSK MODULATION

In this section, the mean BER of the uncoded opportunistic transmission considering BPSK modulation is derived.

From (9) and (10), this mean BER is obtained as

$$\overline{P_b} = \int_{\mathcal{T}}^{\infty} \frac{1}{2}\operatorname{erfc}\left(\alpha_c^2 \frac{E_b}{N_0}\right) \frac{\alpha_c}{\sigma^2} \exp\left(-\frac{\alpha_c^2 + \mathcal{T}^2}{2\sigma^2}\right) d\alpha_c$$
$$= q \int_{\mathcal{T}}^{\infty} \frac{1}{2}\operatorname{erfc}\left(\alpha_c^2 \frac{E_b}{N_0}\right) \frac{\alpha_c}{\sigma^2} \exp\left(-\frac{\alpha_c^2}{2\sigma^2}\right) d\alpha_c, \quad (43)$$

where (7) has been employed. The above integral has a closed-form and as a consequence, (43) can be rewritten as

$$\overline{P_b} = \sigma^2 \left(1 + 2\sigma^2 \frac{E_b}{N_0}\right)^{-\frac{3}{2}} \left\{ \frac{1}{q}\sqrt{2\sigma^2 \frac{E_b}{N_0}} \left(1 + 2\sigma^2 \frac{E_b}{N_0}\right) \times \operatorname{erf}\left(\mathcal{T}\sqrt{\frac{1}{2\sigma^2} + \frac{E_b}{N_0}}\right) + \sqrt{1 + 2\sigma^2 \frac{E_b}{N_0}} \times \left[\left(1 + 2\sigma^2 \frac{E_b}{N_0}\right) \operatorname{erfc}\left(\mathcal{T}\sqrt{\frac{E_b}{N_0}}\right) - \frac{1}{q}\sqrt{2\sigma^2 \frac{E_b}{N_0}\left(1 + 2\sigma^2 \frac{E_b}{N_0}\right)} \right] \right\}, \quad (44)$$

where (7) has been employed and $\operatorname{erf}(x)$ denotes the error function, which is given by $\operatorname{erf}(x) = 1 - \operatorname{erfc}(x)$. The mean SNR has been defined in (12). Employing this definition, with $M = 2$ for BPSK, and after some simplifications, (44) can be rewritten as (13), which is the mean BER expression for uncoded opportunistic transmission schemes considering BPSK modulation.

APPENDIX B
ASYMPTOTIC APPROXIMATION FOR THE COMPLEMENTARY ERROR FUNCTION

An approximation for the complementary error function, defined by (11), is obtained in this appendix considering the high SNR region.

Unfortunately, the integral defined by (11) cannot be evaluated in closed form in terms of elementary functions. However, by employing a recursive process, it is possible to write the complementary error function as a series. Below we detail some steps of this process.

Rewriting (11) as

$$\operatorname{erfc}(x) = \frac{2}{\sqrt{\pi}} \underbrace{\int_x^{\infty} \frac{1}{y} \exp(-y^2) y\, dy}_{\mathcal{I}}, \quad (45)$$

it is possible to integrate by parts by letting $u = 1/y$, $du = -y^{-2}$, $dv = \exp(-y^2)ydy$ and $v = -\exp(-y^2)/2$. Therefore,

$$\mathcal{I} = uv\Big|_x^{\infty} - \int_x^{\infty} v du$$
$$= \frac{1}{2x}\exp\left(-x^2\right) - \frac{1}{2}\int_x^{\infty} \frac{1}{y^2}\exp\left(-y^2\right) dy$$
$$= \frac{1}{2x}\exp\left(-x^2\right) - \frac{1}{2}\underbrace{\int_x^{\infty} \frac{1}{y^3}\exp\left(-y^2\right) ydy}_{\mathcal{J}}. \quad (46)$$

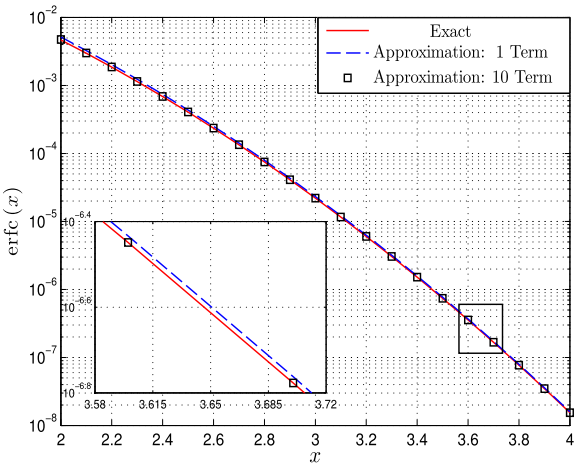

FIGURE 11. Complementary error function approximation.

Similarly, $\mathcal{J}$ can be integrated by parts by letting $u = 1/y^3$, $du = -3y^{-4}$, $dv = \exp(-y^2)ydy$ and $v = -\exp(-y^2)/2$. Hence,

$$\mathcal{J} = \frac{1}{2x^3}\exp\left(-x^2\right) - \frac{3}{2}\int_x^{\infty} \frac{1}{y^4}\exp\left(-y^2\right) dy \quad (47)$$

With (46) and (47), (45) is rewritten as

$$\operatorname{erfc}(x) = \frac{1}{\sqrt{\pi}}\left[\frac{1}{x}\exp\left(-x^2\right) - \frac{1}{2x^3}\exp\left(-x^2\right) + \frac{3}{2}\int_x^{\infty} \frac{1}{y^4}\exp\left(-y^2\right) dy\right]. \quad (48)$$

Repeating the previous process an infinite number of times yields

$$\operatorname{erfc}(x) = \frac{1}{x\sqrt{\pi}}\exp\left(-x^2\right) \times \left[1 + \sum_{\kappa=1}^{\infty}(-1)^{\kappa} \frac{1 \times 3 \times 5 \times \cdots \times (2\kappa - 1)}{(2x^2)^{\kappa}}\right]. \quad (49)$$

For large x, the first term in the above series is the dominant. Hence, this term can be considered as an asymptotic approximation for the complementary error function, that is given by (14). To prove this, Fig. 11 shows the exact $\operatorname{erfc}(x)$ function together with approximations considering 1 and 10 terms of the series given by (49). A region has been amplified in order to observe the results better.

REFERENCES

[1] T. S. Rappaport, *Wireless Communications: Principles and Practice*. Upper Saddle River, NJ, USA: Prentice-Hall, 1996.

[2] H. C. Mora, N. O. Garzón, and C. Almeida, "On the cellular spectral efficiency of MC-CDMA systems with MMSE multiuser detector employing fractional and soft frequency reuse," *AEU-Int. J. Electron. Commun.*, vol. 84, nos. 34–45, Feb. 2018.

[3] Y. Mouchtak, F. El Bouanani, and D. B. da Costa, "A tighter upper bound for the BER of convolutional codes over exponentially correlated Nakagami-m fading," in *Proc. IEEE 29th Annu. Int. Symp. Pers., Indoor Mobile Radio Commun. (PIMRC)*, Sep. 2018, pp. 1–7.

[4] W. C. Huffman and V. Pless, *Fundamentals of Error-Correcting Codes*. New York, NY, USA: Cambridge Univ. Press, 2003.
[5] I. Debbabi, B. Le Gal, N. Khouja, F. Tlili, and C. Jego, "Real time LP decoding of LDPC codes for high correction performance applications," *IEEE Wireless Commun. Lett.*, vol. 5, no. 6, pp. 676–679, Dec. 2016.
[6] T. Zeng, L. Meng, J. Li, M. Luo, X. Li, and L. Huang, "Real time coherent transceiver based on 12-bits 24 dimensions Golay coded modulation," in *Proc. Eur. Conf. Opt. Commun. (ECOC)*, Sep. 2018, pp. 1–3.
[7] N. Benvenuto, L. Bettella, and R. Marchesani, "Performance of the Viterbi algorithm for interleaved convolutional codes," *IEEE Trans. Veh. Technol.*, vol. 47, no. 3, pp. 919–923, Aug. 1998.
[8] A. Desiraju, M. Torlak, and M. Saquib, "Multiple-attempt decoding of convolutional codes over Rayleigh channels," *IEEE Trans. Veh. Technol.*, vol. 64, no. 8, pp. 3426–3439, Aug. 2015.
[9] D. Napp, R. Pinto, and M. Toste, "Column distances of convolutional codes over $\mathbb{Z}_p^r$," *IEEE Trans. Inf. Theory*, vol. 65, no. 2, pp. 1063–1071, Feb. 2019.
[10] D. Divsalar and E. Biglieri, "Upper bounds to error probabilities of coded systems over AWGN and fading channels," in *Proc. Global Telecommun. Conf. (GLOBECOM)*, Nov./Dec. 2000, pp. 1605–1610.
[11] K. Q. T. Zhang, *Wireless Communications: Principles, Theory and Methodology*. Hoboken, NJ, USA: Wiley, 2015.
[12] X. Xiao, Y. Hong, E. Viterbo, and A. Gupta, "Trellis coded modulation for informed receivers," in *Proc. IEEE Int. Conf. Commun. Workshops (ICC-Workshops)*, May 2017, pp. 955–960.
[13] S. Lin and D. J. Costello, *Error Control Coding: Fundamentals and Applications*, 2nd ed. Upper Saddle River, NJ, USA: Prentice-Hall, 2004.
[14] H. R. Ahamed and H. M. Elkamchouchi, "Improving bit error rate of STBC-OFDM using convolutional and turbo codes over Nakagami-m fading channel for BPSK modulation," in *Proc. Int. Conf. Consum. Electron., Commun. Netw. (CECNet)*, Apr. 2011, pp. 4140–4143.
[15] T. Agrawal, A. Kumar, and S. K. Saraswat, "Comparative analysis of convolutional codes based on ML decoding," in *Proc. 2nd Int. Conf. Commun. Control Intell. Syst. (CCIS)*, Nov. 2016, pp. 41–45.
[16] M. N. Meghana, B. R. Reddy, and B. K. Prasad, "Comparitive analysis of channel coding using BPSK modulation," in *Proc. 2nd IEEE Int. Conf. Recent Trends Electron., Inf. Commun. Technol. (RTEICT)*, May 2017, pp. 1354–1358.
[17] S. Weithoffer, C. A. Nour, N. Wehn, C. Douillard, and C. Berrou, "25 years of turbo codes: From Mb/s to beyond 100 Gb/s," in *Proc. IEEE 10th Int. Symp. Turbo Codes Iterative Inf. Process. (ISTC)*, Dec. 2018, pp. 1–6.
[18] J. Li, S. Lin, K. Abdel-Ghaffar, W. E. Ryan, and D. J. Costello, Jr., *LDPC Code Designs, Constructions, and Unification*. Cambridge, U.K.: Cambridge Univ. Press, 2016.
[19] E. Arıkan, "Channel polarization: A method for constructing capacity-achieving codes for symmetric binary-input memoryless channels," *IEEE Trans. Inf. Theory*, vol. 55, no. 7, pp. 3051–3073, Jul. 2009.
[20] T. Wang, D. M. Qu, and T. Jiang, "Parity-check-concatenated polar codes," *IEEE Commun. Lett.*, vol. 20, no. 12, pp. 2342–2345, Sep. 2016.
[21] A. Gupta, M. E. Scholar, A. Jain, and P. D. Vyavahare, "Analysis of error correcting capability of LDPC code over fading and non-fading channel under various parameters," in *Proc. 8th Int. Conf. Comput., Commun. Netw. Technol. (ICCCNT)*, Jul. 2017, pp. 1–5.
[22] O. İşcan, R. Böhnke, and W. Xu, "Shaped polar codes for higher order modulation," *IEEE Commun. Lett.*, vol. 22, no. 2, pp. 252–255, Feb. 2018.
[23] A. A. Giordano and A. H. Levesque, *Modeling of Digital Communication Systems Using SIMULINK*. Hoboken, NJ, USA: Wiley, 2015.
[24] B. Di, L. Song, Y. Li, and S. Zhang, "Trellis coded modulation for code-domain non-orthogonal multiple access networks," in *Proc. IEEE Int. Conf. Commun. (ICC)*, May 2018, pp. 1–6.
[25] B. Di, L. Song, Y. Li, and G. Y. Li, "TCM-NOMA: Joint multi-user codeword design and detection in trellis-coded modulation-based NOMA for beyond 5G," *IEEE J. Sel. Topics Signal Process.*, vol. 13, no. 3, pp. 766–780, Jun. 2019. doi: 10.1109/JSTSP.2019.2899500.
[26] G. N. Orozco and C. de Almeida, "Performance evaluation of opportunistic wireless transmission in Rayleigh fading channels with co-channel interference," in *Proc. IEEE Latin-Amer. Conf. Commun. (LATINCOM)*, Nov. 2013, pp. 1–6.
[27] S. Haykin, "Cognitive radio: Brain-empowered wireless communications," *IEEE J. Sel. Areas Commun.*, vol. 23, no. 2, pp. 201–220, Feb. 2005.
[28] Q. Zhao and L. Tong, "Distributed opportunistic transmission for wireless sensor networks," in *Proc. IEEE Int. Conf. Acoust., Speech, Signal Process.*, May 2004, p. III-833.
[29] N. V. O. Garzon, H. R. C. Mora, and C. de Almeida, "Performance analysis of opportunistic systems employing maximal ratio combining and antenna array," in *Proc. IEEE 84th Veh. Technol. Conf. (VTC-Fall)*, Sep. 2016, pp. 1–5.
[30] H. Nam, K. S. Ko, I. Bang, and B. C. Jung, "Achievable rate analysis of opportunistic transmission in bursty interference networks," *IEEE Commun. Lett.*, vol. 22, no. 3, pp. 654–657, Mar. 2018.
[31] G. G. Messier, "Opportunistic transmission using large scale channel effects," *IEEE Trans. Commun.*, vol. 58, no. 11, pp. 3110–3114, Nov. 2010.
[32] Y. Zou, B. Zheng, and W.-P. Zhu, "An opportunistic cooperation scheme and its BER analysis," *IEEE Trans. Wireless Commun.*, vol. 8, no. 9, pp. 4492–4497, Sep. 2009.
[33] J. P. Woodard and L. Hanzo, "Comparative study of turbo decoding techniques: An overview," *IEEE Trans. Veh. Technol.*, vol. 49, no. 6, pp. 2208–2233, Nov. 2000.
[34] E. Biglieri, D. Divsalar, P. J. McLane, and M. K. Simon, *Introduction to Trellis-Coded Modulation With Applications*. New York, NY, USA: Macmillan, 1991.
[35] C. Berrou, A. Glavieux, and P. Thitimajshima, "Near Shannon limit error-correcting coding and decoding: Turbo-codes. 1," in *Proc. Int. Conf. Commun.*, May 1993, pp. 1064–1070.
[36] A. Bhise and P. D. Vyavahare, "Improved low complexity hybrid turbo codes and their performance analysis," *IEEE Trans. Commun.*, vol. 58, no. 6, pp. 1620–1622, Jun. 2010.
[37] I. Shubhi and Y. Sanada, "Performance of turbo codes in overloaded MIMO-OFDM systems using joint decoding," in *Proc. IEEE 25th Annu. Int. Symp. Pers., Indoor, Mobile Radio Commun. (PIMRC)*, Sep. 2014, pp. 386–390.
[38] B. Tahir, S. Schwarz, and M. Rupp, "BER comparison between convolutional, Turbo, LDPC, and Polar codes," in *Proc. 24th Int. Conf. Telecommun. (ICT)*, May 2017, pp. 1–7.
[39] G. R. Rao and G. S. Rao, "TURBO coded OFDM performance analysis for digital video broadcasting," in *Proc. Int. Conf. Trends Electron. Inform. (ICEI)*, May 2017, pp. 558–560.
[40] A. Papoulis, *Probability—Random Variables and Stochastic Processes*, 4th ed. New York, NY, USA: McGraw-Hill, 2002.
[41] J. K. Cavers and P. Ho, "Analysis of the error performance of trellis-coded modulations in Rayleigh-fading channels," *IEEE Trans. Commun.*, vol. 40, no. 1, pp. 74–83, Jan. 1992.
[42] L. Hanzo, T. H. Liew, and B. L. Yeap, *Turbo Coding, Turbo Equalisation and Space-Time Coding: For Transmission over Fading Channels*. Hoboken, NJ, USA: Wiley, 2002.
[43] J. R. Barry, E. A. Lee, and D. G. Messerschmitt, *Digital Communications*, 3th ed. New York, NY, USA: Springer, 2004.
[44] J. Proakis, "Probabilities of error for adaptive reception of M-phase signals," *IEEE Trans. Commun. Technol.*, vol. COM-16, no. 1, pp. 71–81, Feb. 1968.
[45] D. Divsalar and M. K. Simon, "The design of trellis coded MPSK for fading channels: Performance criteria," *IEEE Trans. Commun.*, vol. COM-36, no. 9, pp. 1004–1012, Sep. 1988.

NATHALY OROZCO GARZÓN received the degree in electronic and telecommunications engineering from Armed Forces University-ESPE, Sangolquí, Ecuador, in 2011, and the M.Sc. and Ph.D. degrees in electrical engineering from the University of Campinas (UNICAMP), Brazil, in 2014 and 2018, respectively. She is currently a Full Professor with the Universidad de Las Américas (UDLA), Quito, Ecuador. Her research interests include digital communications with specific emphasis on multiple access techniques, fading channels, opportunistic systems, and 5G technologies.

HENRY CARVAJAL MORA received the B.Sc. degree in electronics and telecommunications engineering from the Armed Forces University-ESPE, Sangolquí, Ecuador, in 2009, and the M.Sc. and Ph.D. degrees in electrical engineering from the School of Electrical and Computer Engineering (FEEC), University of Campinas (UNICAMP), Brazil, in 2014 and 2018, respectively. He was ranked first in his undergraduate program. In 2018, he was the Director of the Technology Transfer Area with the Education, Science, Technology, and Innovation Secretariat (SENESCYT), Ecuador. He is currently a Full Professor with the Universidad de Las Américas (UDLA), Quito, Ecuador. His research interests include diversity-combining systems, multiple access systems, multiuser detection, MIMO systems, and 5G communications systems.

CELSO DE ALMEIDA received the degree in electrical engineering, and the M.Sc. and Ph.D. degrees from the State University of Campinas (UNICAMP), Brazil, in 1980, 1983, and 1990, respectively, where he joined the Electrical Engineering Faculty, in 1990, and he is currently a Full Professor. He was an Electrical Engineer in optical communications with the industry, from 1982 to 1990. His research interests include cellular systems, CDMA, OFDMA, multiuser detection, antenna arrays, MIMO systems, wireless communications, cryptography, and error correction codes.